



Response surface methodology for optimization of ZIF-8 Synthesis conditions to enhance its removing capability for Pb(II) in aqueous solutions

Gongduan Fan^{a,b,c,*}, Jing Luo^a, Israel de Jesus Lopez Prieto^c, Rujing Lin^a, Xiaomei Zheng^a, Liang Hong^a

^aCollege of Civil Engineering, Fuzhou University, 350116 Fujian, China, email: fgdfz@fzu.edu.cn (G. Fan), Tel. 0086-591-22865361, Fax 0086-591-22865355, email: n160527035@fzu.edu.cn (J. Luo), Tel. 0086-591-22865361, Fax 0086-591-22865355, email: n140527020@fzu.edu.cn (R. Lin), Tel. 0086-591-22865361, Fax 0086-591-22865355, email: n160520053@fzu.edu.cn (X. Zheng), Tel. 0086-591-22865361, Fax 0086-591-22865355, email: n170520050@fzu.edu.cn (L. Hong)

^bInstitute of Advanced Energy Materials, Fuzhou University, 350002 Fujian, China

^cDepartment of Chemical & Environmental Engineering, University of Arizona, 1133 E James E Rogers Way, Harshbarger 108, Tucson, AZ 85721, USA, Tel. 1 (520) 6212573, Fax 1 (520) 621 2573, email: ilopezp@email.arizona.edu

Received 18 March 2018; Accepted 17 September 2018

ABSTRACT

The synthesis conditions of zeolitic imidazolate framework-8 (ZIF-8) have been optimized by a response surface method using central composite design (CCD) to obtain the high adsorption capability for the Pb(II) removal in aqueous solution. The physic-chemical properties of the as-prepared ZIF-8, such as morphology, structure and chemical composition, were characterized by field emission scanning electron microscopy (FE-SEM), powder X-ray diffraction (XRD) and energy-dispersive X-ray photoelectron spectroscopy (XPS), respectively. The adsorption capability, influence factors, isotherms, thermodynamics, kinetics and mechanism of Pb(II) in aqueous solutions were investigated. The optimal parameters of which have the highest adsorption capability for Pb(II) were 200 mL of water as the solvent, and the molar mass ratio of 2-methylimidazole and $Zn(NO_3)_2 \cdot 6H_2O$ was 45.63. At this condition, the as-prepared ZIF-8 was a pure hexagonal three-dimensional crystal structure. The equilibrium adsorption capacity up to 668 mg/g for 300 mg/L of initial Pb(II) solutions and the adsorption was a spontaneous process. The largest adsorption capacity from Langmuir isotherm model was 686.25 mg/g. The adsorption kinetics followed the pseudo-second-order model. The equilibrium adsorption time and the optimal adsorption pH was 4 h and 6.0–7.0, respectively. The ZIF-8 still kept well adsorption effect after three times of usage. Therefore, this study showed that ZIF-8 is a promising sorbent for removing environmental pollutants.

Keywords: Zeolitic imidazolate framework-8 (ZIF-8); Lead; Response surface methodology; Adsorption capability; Influence factor

1. Introduction

With the rapid promotion of industrialization and urbanization progress, quantities of wastewater containing toxic substances has been discharged into the environment directly [1]. This wastewater containing heavy ions is not only harmful to the environment, but also can cause a series of diseases threatening human health, such as cancer. Different from organic pollutants, heavy metal

ions are not only hard to biodegrade, but also easy to accumulate in biological body [2] and the lead (Pb(II)) is one of the representatives. Pb(II) is a non-essential element for humans [3]. An overdose in the consumption lead will cause anaemia, insomnia, and even lead to kidney failure or other diseases. Therefore, it is urgent to find an effective method to treat the water polluted by Pb(II) [4].

Heavy metal ions usually are removed by chemical precipitation, ion exchange, reverse osmosis or adsorption. Chemical precipitation is the most prevalent among them. However, comparing with chemical precipitation,

*Corresponding author.

adsorption is more suitable for low concentration [5]. Adsorption is a simple technology yet a highly effective and low-cost method to remove pollutants from water [6–10]. Mohammadi et al. [11] used peach shell activated carbon to adsorb Pb(II) and the equilibrium adsorption capacity was 36.36 mg/g. These types of adsorbents have lower prices and wider sources, but they have poor selection and low adsorption capacity. Morsy [12] used the hydroxyl apatite gel biological adsorbents to remove Pb(II) from wastewater. These adsorbents have large adsorption capacity which up to 334.8 mg/g, but their lifetime was unsatisfactory. Hence, it is critical to find appropriate adsorbents with large adsorption capacity and good stability.

In recent years, zeolitic imidazolate frameworks (ZIFs) have attracted great attention due to their excellent properties including high thermal stability, large specific surface area, high porosity and so on. ZIF-8 is one of the most popular metal organic frameworks (MOFs) due to the hydrophobicity and well chemical stability in aqueous phase adsorption [13–15]. With more and more heavy metal polluting events, removal of heavy metal in polluted water is significant. However, the removal of heavy metal by ZIF-8 is still in an early stage. As we know, the synthesis conditions will greatly influence the adsorption capability of materials. In other words, the synthesis conditions will determine the adsorption capability of materials, but very few researches give the relation between the synthesis conditions and adsorption capability of materials directly.

In this paper, we used heavy metal ions Pb(II) as the representative pollutants and ZIF-8 as adsorbents. The synthetic conditions of ZIF-8 were optimized by using an optimal experimental design based on central composite design (CCD) to enhance its removing capability. The adsorption process are explored through adsorption kinetics model, adsorption isotherm model and thermodynamics model. The adsorption mechanism of Pb(II) on ZIF-8 surface and the effects of environmental factors to adsorbent efficiency were also investigated. All above studies would provide some theoretical and technical supports in the removal of Pb(II) from water in practical application.

2. Materials and methods

2.1. Materials and main instruments

$Zn(NO_3)_2 \cdot 6H_2O$, NaOH, HCl, $Pb(NO_3)_2$, $Ni(NO_3)_2$ and $CuCl_2$ were purchased from Sinopharm and 2-methylimidazole was purchased from Aladdin. All reagents were analytical grade purity except the standard stock solution of Pb (1000 mg/L) was guaranteed reagent. For preparing the Pb(II) ions solution, weighted $Pb(NO_3)_2$ was dissolved by deionized water to 2000 mg/L and further diluted for the required experiments.

Main instruments containing Ultima IV X-ray power diffraction (XRD, Rigaku. Co. Ltd, Japan), field emission scanning electron microscope (FE-SEM, S-4800, Hitachi. Ltd, Japan), high-resolution transmission electron microscopy (HRTEM, TECNAL G2F20, FEI Company, USA), Fourier transform infrared spectroscopy (FT-IR, Nicolet 6700, Thermo Fisher Scientific. Co. Ltd USA), water bath thermostatic oscillator incubator (SHA-C, Changzhou Guohua Electric Appliances Ltd, China) pH

meter (pH-201, HANNA Co. Ltd. Italy), super centrifuge (Mikro 22R Hettich Co. Ltd. Germany), inductively coupled plasma optical emission spectrometer (ICP-OES, OPTIMA 8000, Perkin-Elmer Co. Ltd. USA), X-ray photoelectron spectroscopy (XPS, ESCALAB250, Thermo Fisher Scientific, USA) Zeta potential analyzer (Nano ZS90, UK) and so on were used in this study.

2.2. Synthesis and characterization of ZIF-8

ZIF-8 was synthesized by a simple modified stirring method using $Zn(NO_3)_2 \cdot 6H_2O$ (Sinopharm Chemical Reagent) and 2-methylimidazole (Aladdin Reagent) as the raw materials [16]. 1.0 g of $Zn(NO_3)_2 \cdot 6H_2O$ and specific dosage (5.5, 11.05 or 16.6 g) of 2-Methylimidazole were dissolved in specific volume (100, 150 or 200 mL) of deionized water, respectively. Then, two solutions were mixed at room temperature under stirring for 1 h followed by filtrating the milk-like suspensions and then washed the precipitation with deionized water three times. Finally, the white products were dried in oven at 70°C for a whole night and collected for reserve.

Finally, the as-prepared samples and the samples which Pb(II) adsorbed on were grinded. The phases compositions of these samples were then analyzed by XRD using Cu K α radiation ($\lambda = 1.54059 \text{ \AA}$) with a scanning range of 5–50°. The morphologies of ZIF-8 were investigated by FE-SEM. The infrared spectra of samples, which were prepared by KBr pellet pressing method, were measured by FT-IR with a measurement range and distinguishability of 4000–400 cm^{-1} and 4 cm^{-1} , respectively. Concentration of Pb(II) was measured by ICP-OES before and after the adsorption.

2.3. Optimizing experiment by response surface methodology

Based on one-way experiment design, the two factors investigated were reagent molar mass ratio ($H_{mim} : Zn^{2+}$) and solvent volume, and the adsorption volume were used as the respond value. The central composite response surface experiment was established to obtain the optimized synthesis parameter. The codes and levels of experiment factors are shown in Table 1.

2.4. Batch heavy metal ions adsorption experiments

All batch experiments were carried out in a table concentrator (SHA-C thermostatic oscillator, Guohua Electric Appliance Co. Ltd, Changzhou, China) with a rate

Table 1
Levels and codes of central composite design

Solvent variety	Factors	Codes value	Codes value in all level		
			-1	0	1
Water	Reagent molar ratio of Hmim: Zn^{2+}	A	20	40	60
	Solvent volume (mL)	B	100	150	200

of 200 rpm under $25 \pm 1^\circ\text{C}$ ambient conditions. Specific dosage of ZIF-8 were added to 50 mL of Pb(II) solution with the certain concentration. After a certain amount of contact time, supernatant liquor was filtered through 0.22 μm membrane and diluted to desired volumes.

1. Adsorption experiments of response surface methodology: Pb(II) was 300 mg/L, the dosage of ZIF-8 was 0.2 g/L, the temperature was $25 \pm 0.1^\circ\text{C}$ and pH was 4.5 ± 0.1 , the experiments were carried out in a table concentrator with 180 min.
2. The effects of adsorbing time: The initial concentration of Pb (II) was 200 mg/L, the dosage of ZIF-8 was 0.2 g/L, the pH was 4.5 ± 0.1 and the temperature was $25 \pm 0.1^\circ\text{C}$. The sampling interval time was 0, 3, 10, 20, 40, 60, 80, 120, 180, 240, 300, 420 and 510 min, respectively.
3. The effects of initial heavy metal ions concentration: The dosage of ZIF-8 was 0.2 g/L, the temperature was $25 \pm 0.1^\circ\text{C}$, the oscillating time was 240 min, pH was 4.5 ± 0.1 . The initial heavy metal ions concentrations were 10, 20, 50, 100, 200, 300, 400, 700, 1000 and 1500 mg/L, respectively.
4. The effects of pH: The initial concentration of Pb(II) was 200 mg/L, the dosage of ZIF-8 was 0.2 g/L, temperature was $25 \pm 0.1^\circ\text{C}$, the oscillating time was 240 min, and the initial pH of Pb(II) solution was adjusted to 2.0, 3.0, 4.0, 5.0, 6.0, 7.0, 8.0 and 9.0 individually by using dilute HCl or NaOH (0.1 M).
5. The effects of adsorbent dosage: The initial concentration of Pb(II) was 200 mg/L, the temperature was $25 \pm 0.1^\circ\text{C}$, the oscillating time was 240 min, the solution pH was 4.5 ± 0.1 , the dosage of TNs were 0.05, 0.1, 0.5, 1.0, 1.5, 2.0, 2.5 and 3.5 g/L, respectively.
6. Competitive adsorption: The initial concentration of Pb(II) was 200 mg/L, the dosage of ZIF-8 was 0.2 g/L, the oscillating time was 240 min, the concentration of Cu(II) or Ni(II) was 200 mg/L, respectively.
7. Recycled adsorption: The initial concentration of Pb(II) was 200 mg/L, the dosage of ZIF-8 was 0.2 g/L, the temperature was $25 \pm 0.1^\circ\text{C}$, and the oscillating time was 240 min. After adsorption equilibrium, initial concentration C_0 and equilibrium concentration C_e of heavy metal ions were measured. Adsorbed ZIF-8 was eluted by methyl alcohol. The eluted ZIF-8 was used to adsorb Pb(II) under identical experimental conditions. After adsorption equilibrium, initial concentration C_0 and equilibrium concentration C_e of heavy metal ions were measured again.

The amount of adsorbed metal ions q_t at time t (min), the amount of adsorbed metal ions at equilibrium q_e (mg/g) and the metal ions removal Ratio R (%) were calculated by as follows:

$$q_t = \frac{(C_0 - C_t)V}{m} \quad (1)$$

$$q_e = \frac{(C_0 - C_e)V}{m} \quad (2)$$

$$R = \frac{C_0 - C_e}{C_0} \times 100 \quad (3)$$

where C_0 , C_t and C_e (mg/L) are the initial concentrations, concentrations at time t (min) and the equilibrium concentration of Pb(II), respectively, m (g) is the mass of ZIF-8 and V (L) is the volume of Pb(II) solution.

3. Results and discussion

3.1. Optimal experimental based on response surface methodology

3.1.1. Experimental design and results of central composite

The experiments were designed though different combination of factors by RSM. Experimental design and the results of Central Composite based on ZIF-8, synthesized by water as the solvent, adsorbed and removed Pb(II) in the water are shown in Table 2.

According to the experimental results, data was analyzed through the software of Design Expert 8.0.6 and then got the fitted equation as follows.

$$\text{Adsorption capacity} = 581.14 + 16.61 \times A + 46.00 \times B - 12.31 \times A \times B - 7.68 \times A^2 + 19.15 \times B^2 \quad (4)$$

Significance test and variance analysis of regression equation of ZIF-8, synthesized by water as the solvent, adsorbed and removed Pb(II) in the aqueous solution are shown in the Table 3.

Table 2
Experimental design and the corresponding results

Number	Copes and levels of variable		Adsorption capacity (mg/g)	Predicted adsorption capacity (mg/g)	Errors (observed-predicted) (mg/g)
	A	B			
1	0	-1	556.00	554.29	1.71
2	0	0	575.25	581.14	-5.89
3	0	0	580.50	581.14	-0.64
4	-1	1	634.25	634.31	-0.06
5	0	0	584.25	581.14	3.11
6	1	0	593.75	590.07	3.68
7	1	1	641.00	642.91	-1.91
8	0	0	579.50	581.14	-1.64
9	0	0	582.50	581.14	1.36
10	1	-1	573.75	575.53	-1.78
11	0	1	648.25	646.29	1.96
12	-1	-1	517.75	517.69	0.06
13	-1	0	357.50	556.85	-199.35

Table 3
Analysis of variance (ANOVA)

Items	Quadratic sum	Degree of freedom	Mean square	F-value	P-value Prob > F	Remark
Model	15022.61	5	3004.52	235.82	<0.0001	Remarkable
A	1244.74	1	1244.74	97.70	<0.0001	
B	12696.00	1	12696.00	996.49	<0.0001	
AB	606.39	1	606.39	47.59	0.0005	
A ²	119.20	1	119.20	9.36	0.0223	
B ²	768.19	1	768.19	60.29	0.0002	
Error	76.44	6	12.74			
Lack of fit	29.87	2	14.93	1.28	0.3712	Non-significant
Pure error	46.58	4	11.64			
Sum	15099.06	11				

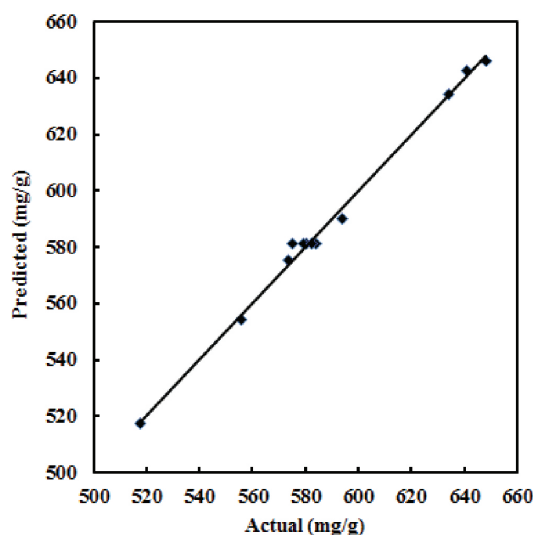


Fig. 1. Comparison of the predicted and actual value of adsorption capability.

The significance of regression Quadratic models in terms of ANOVA. *F*-value of model can reach to 235.82 and *P*-value < 0.0001. It indicates that this model reached a dramatic level, which means that this model has reasonable fitted effect in this research area. The determination coefficient $R^2 = 0.9949 > 0.95$. It indicates that changes of responded value can be responded by this model under the range of 99.49%. Comparison of the predicted value and real value of adsorption capacity are shown in Fig. 1. As shown in Fig. 1, the predicted and real value are essentially on the same line, indicating the predicted results of this model are highly consistent with experimental measurement results. Therefore, this model can be used to analyze and predict Pb(II) removal process by ZIF-8, using water as the solvent, in a specific range because of its strong correlation. $R_{adj}^2 - R_{pred}^2 = 0.9907 - 0.9769 = 0.0138 < 0.2$, C.V. = 0.61% < 10%, it reveals that this experiment has high reliability

and accuracy. Adeq Precision = 50.950 > 4, it indicates that signal to noise ratio is large and has enough signal response design [17]. Regression coefficient of quadratic regression model was tested for significance. The results shown *P*-value of A, B, AB, B² are all smaller than 0.01 and are extremely significant. *P*-value of A² is smaller than 0.05 and reach significance level. Factor of A and B shows obvious linear effect on adsorption capacity and AB, A² B² shows obvious surface effect.

3.1.2. Double factors interaction effects of the response surface analysis

According to Table 2 and Eq. (1), the mole ratio and solvent volume respond surface and contour line are shown in Fig. 2. It shows that the interaction effects between the mole ratio and solvent volume on adsorption capability. The red areas and blue areas reveal the adsorption capability representing large and small, respectively. The changes of volume capacity can be directly shown by color gradient. As the results of the adsorption of Pb(II) with ZIF-8, adsorption capacity increased first and then decreased with the increase of mole ratio of H_{min} and Zn^{2+} . With the increase of solvent volume, adsorption capacity is greater and contour lines become more intensive, revealing that effects of solvent volume to adsorption capacity gradually become bigger. Reciprocal effects between mole ratio and solvent capacity make it exhibit a high adsorption capacity area, which is the red area in the Fig. 2. The capacity volume is 200 mL and the mole ratio of H_{min} and Zn^{2+} is from 50 to 60 in this area.

According to Design Expert 8.0.6 optimizing, when the dosage of $Zn(NO_3)_2 \cdot 6H_2O$ was 1.0 g, the mole ratio between H_{min} and Zn^{2+} was 45.63, solvent capacity was 200 mL, the predicting adsorption capacity of model reach to 646.89 mg/g. Through experimental confirmation, the real adsorption capacity was 668.00 mg/g for 300 mg/L of initial r Pb(II) solutions, and the error ratio was only 3.26%. It reveals that the fitting effects of the experimental values and the predicted values are well-optimal and well-fitting. Therefore, optimal synthetic parameters of ZIF-8, which was

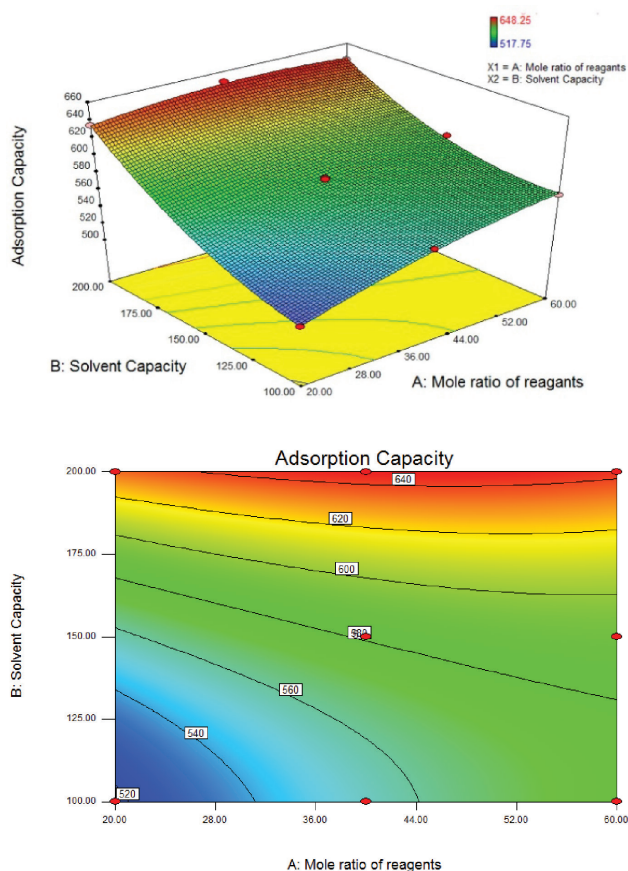


Fig. 2. Response surface (3D) showing reciprocal effects of different parameters on adsorption capability.

synthesized via response surface method, is reliable. It can be used to predict adsorption capacity of ZIF-8 for Pb(II) synthesized in some condition and own some practical value.

3.2. ZIF-8 characterization

3.2.1. XRD analysis

XRD patterns of ZIF-8 before and after adsorption are shown in Fig. 3. Before adsorption, the characteristic peaks of samples are all consistent with reported samples [18], which are $7.31^\circ(011)$, $10.36^\circ(002)$, $12.72^\circ(112)$, $14.40^\circ(022)$, $16.45^\circ(013)$, $18.04^\circ(222)$, $22.15^\circ(114)$, $24.53^\circ(233)$, $25.62^\circ(224)$, $26.70^\circ(134)$, $29.67^\circ(044)$, $30.62^\circ(334)$, $31.55^\circ(244)$ and $32.43^\circ(235)$. The diffraction peaks of synthetic samples were relatively strong indicating a pure ZIF-8 with high degree of crystallinity has been successfully synthesized. After the adsorption, peaks have not obviously changed, which indicates ZIF-8 retained stable framework after adsorbing Pb(II).

3.2.2. Analysis of SEM, TEM and EDS

SEM and TEM patterns of synthetic samples before and after adsorption are shown in Fig. 4. Synthetic samples

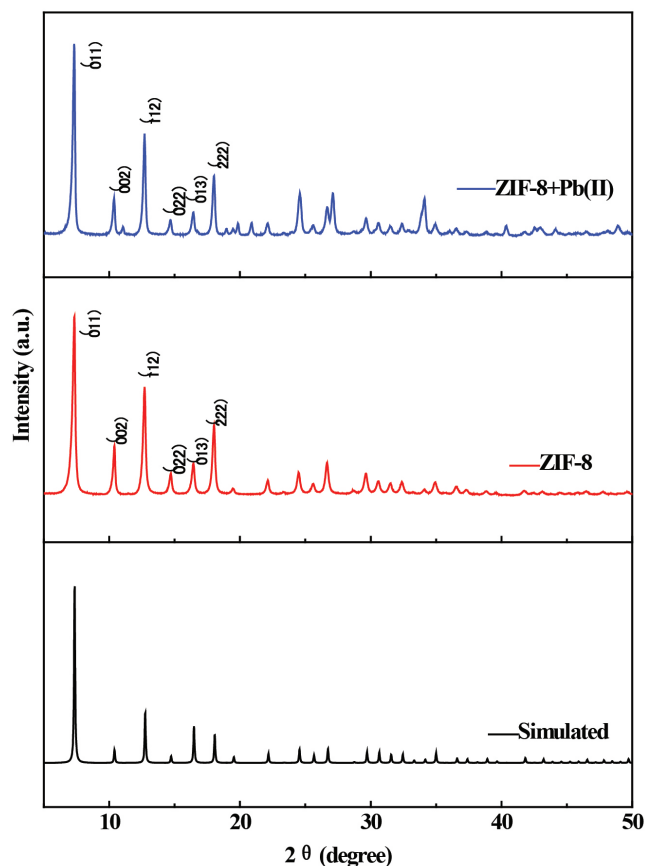


Fig. 3. XRD patterns of ZIF-8 before and after adsorption of Pb(II).

were hexagonal stereo chemical structure in two sides. The particles array closely and morphology was orderly. Crystal granularity was about $1\ \mu\text{m}$. Size and morphology of samples have remained almost unchanged after the adsorption of Pb(II). It reveals that the structure of ZIF-8 has well stability in the adsorption process.

Samples were also analyzed by EDS to understand the changes of surface element before and after adsorption. As shown in Fig. 5, the samples contain peaks of C, N, O, Zn, Al before adsorption, while Al came from sample platform. After adsorption, the peaks of Pb(II) can be obviously found by EDS. This phenomenon indicates ZIF-8 did adsorb Pb(II) on the surface of ZIF-8 in some form.

3.2.3. Analysis of N_2 adsorption–desorption isotherms

The N_2 sorption–desorption isotherms of ZIF-8 is shown in Fig. 6. It can be found out the isotherms of ZIF-8 was a type I isotherm of BDDT (Brunauer–Deming–Deming–Teller) without hysteresis loops, which confirmed the formation of a micropore structure. The data was analyzed while P/P_0 set as 0.05–0.35. The Brunauer–Emmett–Teller (BET) surface area and pore volume of the sample are $1114.5\ \text{m}^2/\text{g}$ and $0.59\ \text{cm}^3/\text{g}$, respectively.

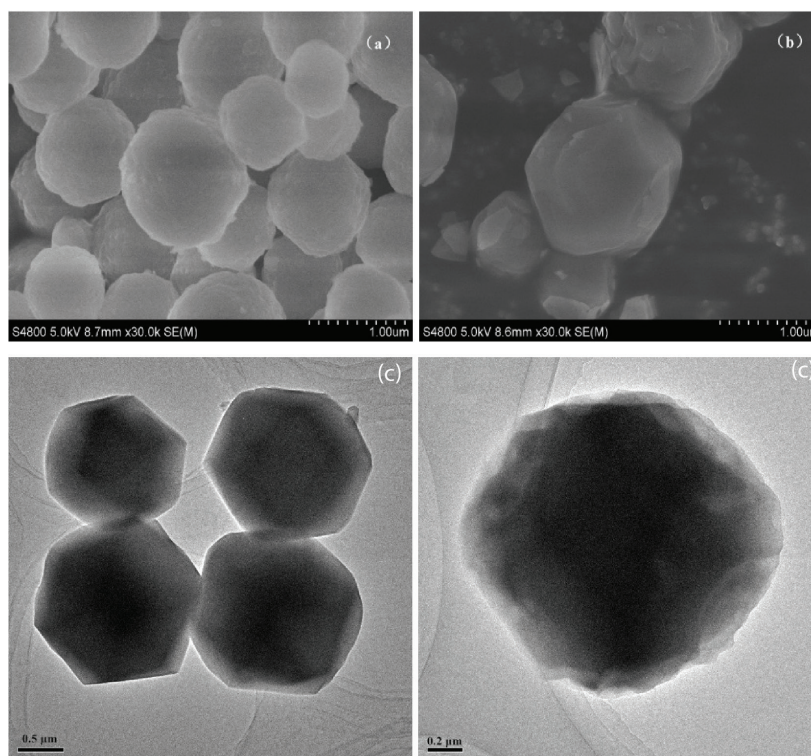


Fig. 4. SEM images of ZIF-8 (a) before and (b) after adsorption of Pb(II), TEM images of ZIF-8 (c) before and (d) after adsorption of Pb(II).

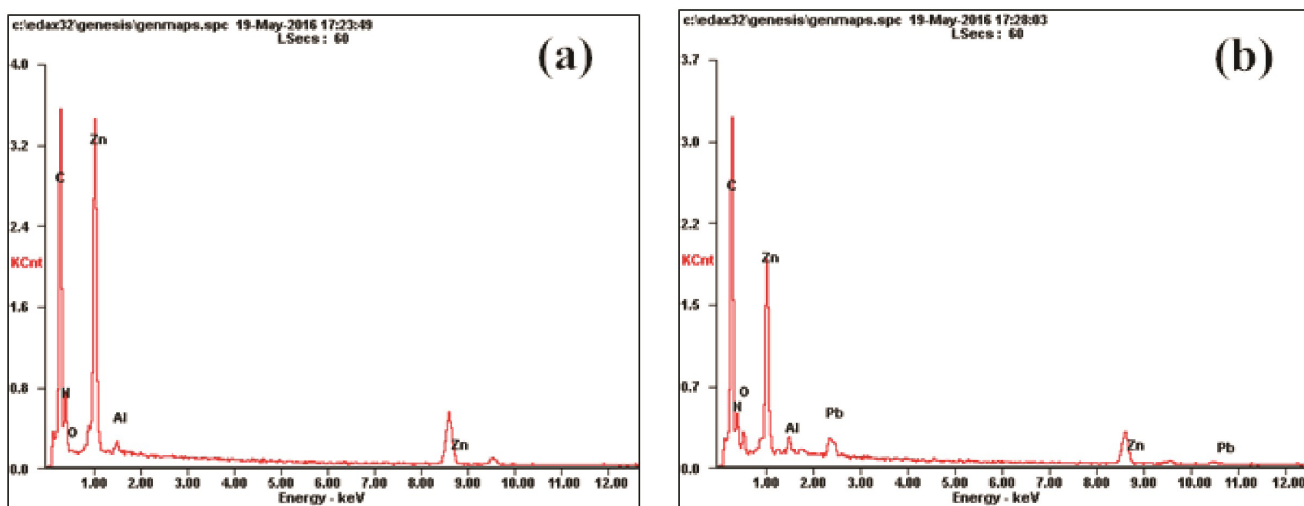


Fig. 5. EDS spectra of ZIF-8 (a) before and (b) after adsorption of Pb(II).

3.3. Experiment of adsorption for Pb(II) by ZIF-8

3.3.1. Effects of adsorption time

The adsorption time is an important parameter for adsorption equilibrium. For decreasing time cost, equilibrium time should be confirmed by studying adsorption time. Changes of adsorption capacity with the increase of time are shown in Fig. 7. It shows that the adsorption process can be divided into three steps. Firstly,

adsorption capacity increases sharply with time within the first 10 min, ultimately reaching 181.50 mg/g at 10 min. On this stage, qualities of active adsorption sites in ZIF-8 surface were occupied by Pb(II) [19], thereby adsorption capacity increased. Secondly, adsorption capacity developed a slowly increasing trend from 10 min to 240 min and the adsorption process enters the last stages after 240 min. Lastly, the adsorption capacity almost remains the same level, which is approximately 446.5 mg/g.

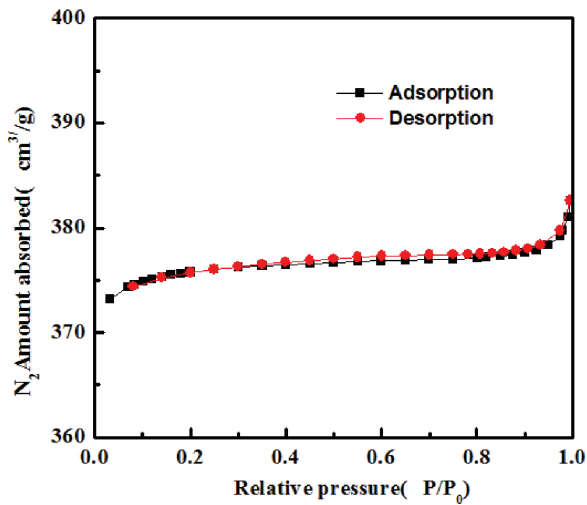


Fig. 6. N_2 adsorption-desorption isotherms of ZIF-8.

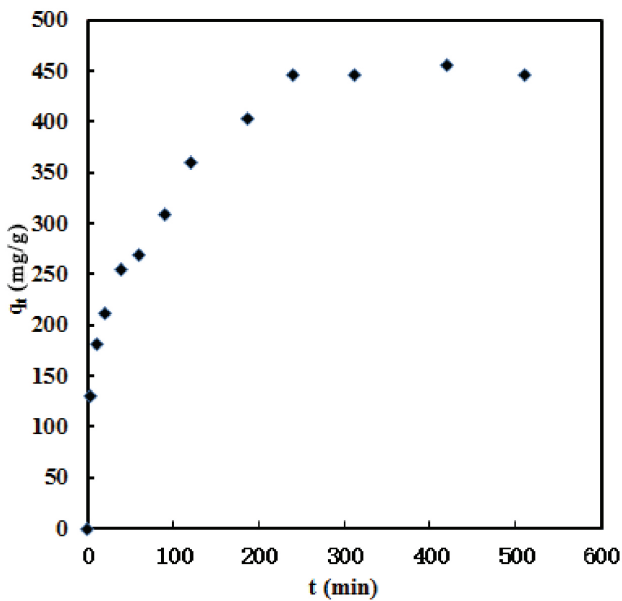


Fig. 7. Effects of contact time on the adsorption of Pb(II) with ZIF-8.

Adsorption reaches equilibrium and adsorption rate decreases due to the generally saturating sites. As shown in Fig. 7, the equilibrium adsorption time was 240 min. Therefore, adsorption time was 240 min in the following experiments.

3.3.2. Effects of pH

The pH will affect adsorption through changing pollutants distribution and interfering with binding sites on sorbent surface [20]. Therefore, this experiment explored the effect of pH on adsorption for Pb(II) with ZIF-8.

When the pH ranged from 2 to 9, the removal ratio of adsorption for Pb(II) (initial concentration 200 mg/L) by ZIF-8 is shown in Fig. 8. It reveals that there is a positive

correlation between removal ratio and pH. When $pH < 4$, the removal ratio was lower than 70%. Especially, when $pH = 2$, the removal ratio was only 29.03%. When the pH was between 4 and 7, removal ratio trended to increase slowly, from 73.37% to 85.21% with the increase of the pH. When $pH > 7$, removal ratio further increased and stabilized at about 90%, because the dissolution of ZIF-8 would significant decrease in acid environment. Fig. 9a shows dissolution amount and dissolution ratio (R_D) of ZIF-8, which were represented by Zn^{2+} , in different pH environments. As shown in Fig. 9a, when $pH < 4$, the acid environment made ZIF-8 dissolve a lot and the dissolution ratio became more than 70%, leading to low adsorption effects of ZIF-8 for Pb(II). With the increase of pH, the amount of dissolved ZIF-8 became lower and lower. When $pH = 7$, dissolved amount was only 5.7 mg/L, so it had good adsorption effects. Because solubility product constant of Pb(II) is 1.2×10^{-15} , theoretical pH of forming precipitated hydroxide of Pb(II) is 8.2 through calculating. Therefore, when the pH further increasing, $Pb(OH)_2$ would form and precipitate, leading to an increase removal ratio. Zeta potential of the ZIF-8 at different pH was illustrated in Fig. 9b. It can be found out that the isoelectric point (pH_{IEP}) is about 8.2. The surface charges of as-prepared ZIF-8 at pH below and above pH_{IEP} are positive and negative, respectively. As Pb(II), the negative charge can be better adsorbed at higher pH. But as shown in Fig. 8, the removal ratio of Pb(II) did not increase at pH 9.0 compared to 8.0. So, the electrostatic attraction did not play a key role in the adsorption process. Optimal pH of adsorption for Pb(II) with ZIF-8 should be controlled between 7.0 and 8.0 for avoiding disturbing adsorption process due to the formation of hydroxide precipitate. In real conditions, maybe we can set the pH between 7.0 and 8.0 to adsorb the heavy metals in aqueous solution, and then set the pH

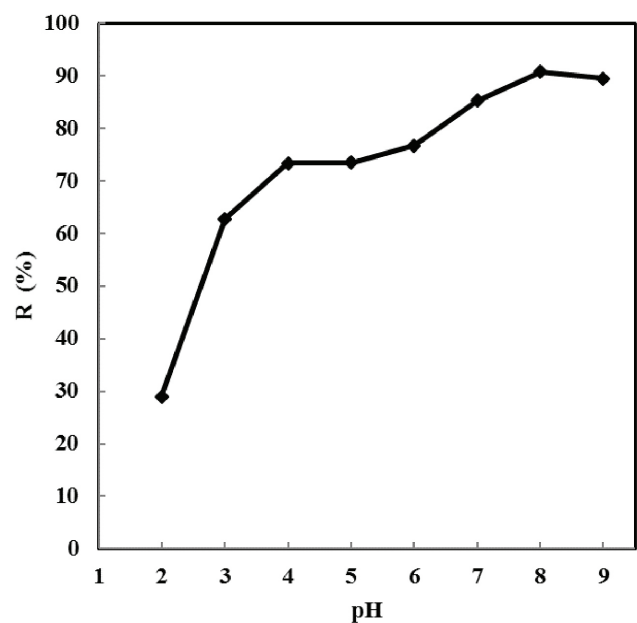


Fig. 8. Effects of pH on adsorption of Pb(II) with ZIF-8.

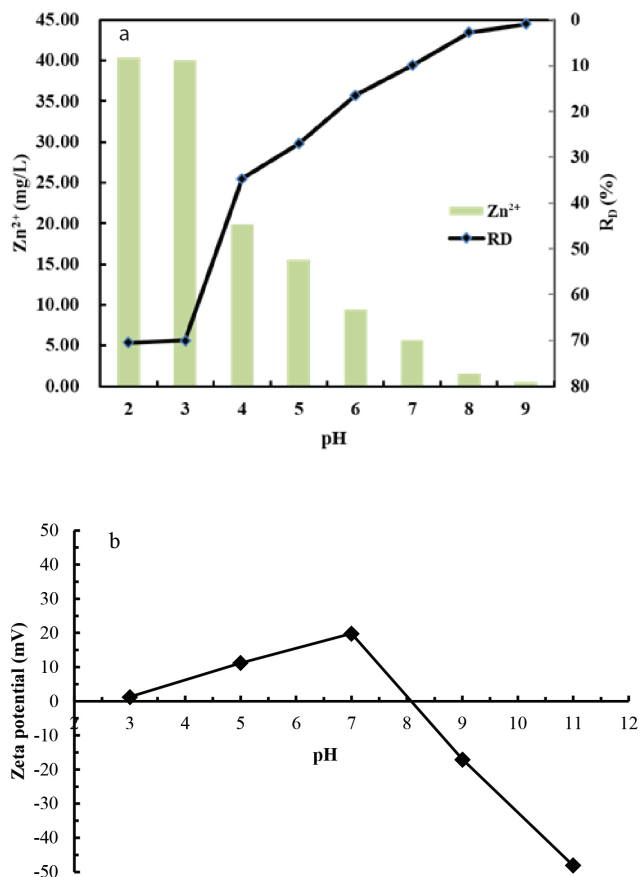


Fig. 9. (a) Effects of solution pH on Zn²⁺ leaching and (b) the zeta potential of the synthesized ZIF-8.

at acid condition to dissolve the adsorbent to recover the heavy metal.

3.3.3. Initial concentration effects of Pb(II)

Initial concentration of pollutants is one of basic parameters which confirm system loading and relate to adsorption effects. Therefore, this experiment explored the effect of initial Pb(II) concentration on adsorption effects. The result is shown in Fig. 10, revealing that equilibrium adsorption capacity increases and removal ratio decreases with the increase of initial concentration. When initial concentration was 10 mg/L, adsorption capacity was 9.03 mg/g and removal ratio reached to 99.29%. When initial concentration reached to 1400 mg/L, adsorption capacity increased to 1176.5 mg/g and removal ratio decreased to 17.33%. Because high initial concentration make metal ions concentration gradient become large. The mass transfer driving force, produced from solid-liquid interface, makes Pb(II) migrate to active sites of surface of the ZIF-8 and causes adsorption capacity to increase. Simultaneously, adsorption capacity of ZIF-8 for Pb(II) is limited. When initial concentration increases to limited value, surface of ZIF-8 would be saturated, which means that more and more Pb(II) won't be adsorbed and the removal ratio of Pb(II) will decrease [21].

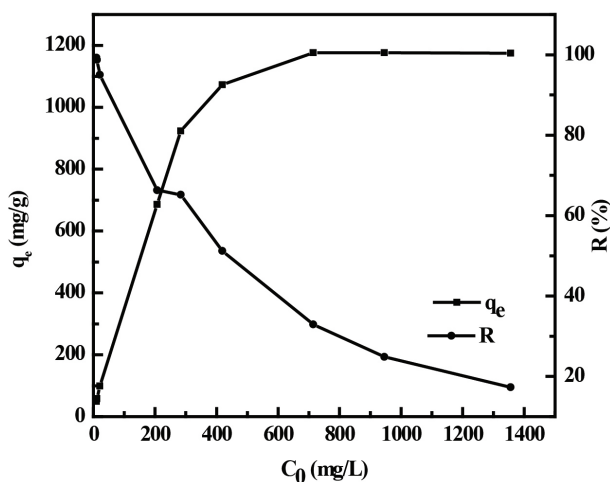


Fig. 10. Effects of initial concentration on the adsorption capacities and removals at equilibrium of Pb(II) by ZIF-8.

3.3.4. Effects of ZIF-8 dosage

Absorbent dosage affects treatment efficiency and cost, thereby the effect of ZIF-8 dosage on adsorption efficiency of Pb(II) was explored. As shown in Fig. 11, when ZIF-8 dosage was 0.05 g/L, the largest adsorption capacity was 1569.00 mg/g, but removal ratio was the lowest, which was 43.02%. When ZIF-8 dosage was between 0.05 g/L and 0.5 g/L, adsorption capacity decreased quickly with the increase of the dosage firstly. Then, the ratio decreased slowly with the further increase of dosage and adsorption capacity stable at 1569.00 mg/g at last. But removal ratio had an increasing trend with dosage increasing, even reaching 92.78% when dosage is 3.5 g/L.

Absorbent dosage, specific surface area of absorbent and amount of absorbent active sites are main factors to influence the adsorption results[22]. When ZIF-8 dosage was less than 0.1g/L, adsorption sites could be fully used in the adsorption process. When dosage was between 0.1 g/L and 3.5 g/L, adsorption sites on ZIF-8 surface couldn't be used fully and the concentration of heavy metal ions

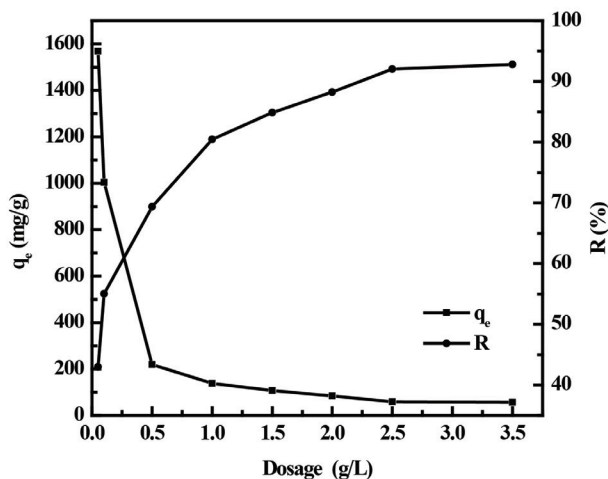


Fig. 11. Effects of dosage on adsorption of Pb(II) by ZIF-8.

decreased on surface of unit mass ZIF-8. However, with the increase of absorbent dosage, the specific surface area and amount of adsorption sites increased meanwhile the removal ratio increased. Therefore, increase the adsorbent dosage would increase the adsorption capacity as well as the removal ratio before adsorption equilibrium.

3.3.5. Effect of competing ion Ni(II) and Cu(II) on sorption

Commonly, there are more than one kind of metal ions in the real polluted water, Various metal ions might interfere with or compete with the Pb(II) adsorption [23]. Therefore, Pb(II) was chosen as target metal ions and Ni(II) and Cu(II) as interference ions. The adsorption effects for Pb(II) is shown in Table 4. The results show that adsorption capacity of ZIF-8 for Pb(II) was lower in the mixed system than the single system. In the single system, adsorption capacity of Pb(II) was 686.25 mg/g,

II) system and Pb(II)+Ni(II) system than single system, respectively. This result reveals that Cu(II), comparing to Ni(II), remarkably inhibits adsorption of Pb(II). In the mixed system of three kinds of ions, adsorption capacity was 27.98% less than in the single system but increased 23.01% more than in the Pb(II) + Cu(II) system. It suggests that Ni(II) will inhibit adsorption of Cu(II) by ZIF-8. The above results reveal that each kind of ion will compete for ZIF-8 adsorption sites and inhibit each other. Therefore, adsorption capacity of target ions will decrease [24].

The above results also show that different ions will compete and restrain each other for active sites of ZIF-8 and decrease the adsorption capacity of target ions. It is reported that selective adsorption of a metal element is related to electronegativity [25]. The metal element of larger electronegativity can form a stronger covalent bond. Besides, ions radius is also related to adsorption capacity. Due to larger ions radius of Pb(II) (1.12 Å) comparing to Cu(II) (0.70 Å), absorbent have more available for Cu(II) [26]. Therefore ZIF-8 will firstly adsorb Cu(II) and have larger adsorption capacity in the Pb(II) + Cu(II) system. However, in the Pb(II) + Ni(II) system and the Pb(II) + Ni(II) + Cu(II) system, adsorption capacity of ZIF-8 for Pb(II) was larger than other ions, so adsorption selection didn't fit electronegativity sorting on this condition. Besides, Heat of hydration of metal is also an important factor to

the absorption of metal. Pb(II) has the smallest heat of hydration, which reveals that bare Pb(II) are immobilized easily due to loss of water ligand.

In conclusion, ions will compete with each other, leading to the decrease of the adsorption capacity for target ions in many kinds of ions system. The adsorption selection of ions is relating to many factors, such as electronegativity, heat of hydration ionic radius, complex stability constant and so on.

3.3.6. Recycled adsorption experiment

Recycling absorbents can make costs lower and extend absorbents work life. Therefore, this experiment used ethyl alcohol [27] and methanol [28] to desorb adsorbed ZIF-8 in pH = 4 condition and recycle ZIF-8. As shown in Fig. 12a, the adsorption capacity of ZIF-8, which was desorbed by ethyl alcohol, only decreases 61.25 mg/g and the decrease ratio of capacity is 8.93% after 3 cycles. This result reveals that desorbed ZIF-8 perform well stability at high adsorption capacity of ZIF-8 for Pb(II). But adsorption capacity of ZIF-8, which was desorbed by methanol, decreases gradually from 686.25 mg/g to 517.25 mg/g and the decrease ratio of capacity is 24.63%. However, ZIF-8 still shows a large adsorption capacity comparing to other materials. In the experiment of Karthik et al. [29], adsorption capacity of Polyaniline grafted chitosan for Pb(II) was just about 16.07 mg/g, just 4% of adsorption capacity of ZIF-8. In another experiment, Zhou [30] and co-workers used EPS

Table 4
Adsorption capability in single metal ion and multiple metal ions adsorption by ZIF-8

Solution system	Heavy metal ions	q_e mg/g
Pb	Pb	686.25
Pb+Ni	Pb	638.00
	Ni	58.50
Pb+Cu	Pb	380.50
	Cu	463.00
Pb+Cu+Ni	Pb	494.25
	Cu	221.25
	Ni	12.25

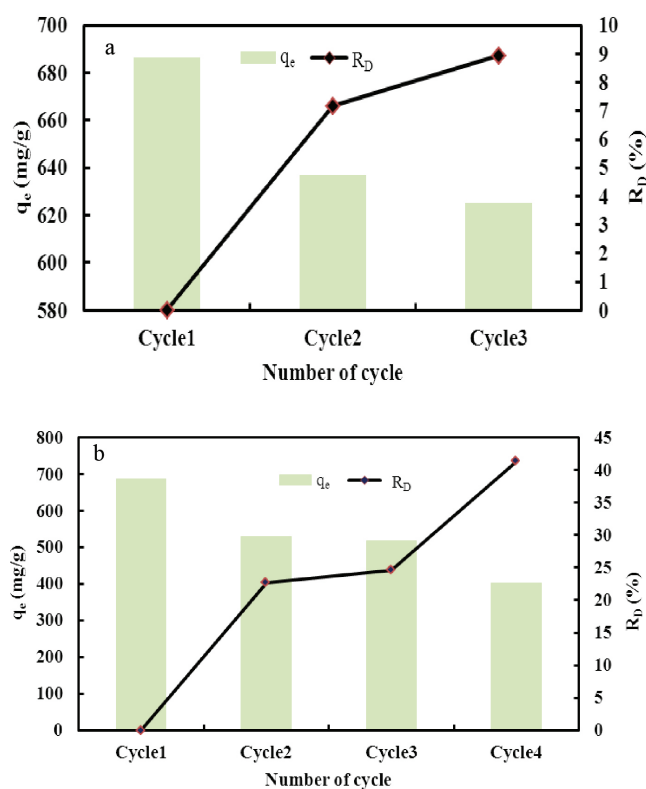


Fig. 12. Reusability of ZIF-8 washed with (a) acidic ethanol and (b) methanol for the adsorption of Pb(II).

of activated sludge as adsorbents, and adsorption capacity was about 208.28 mg/g. It is also less than ZIF-8 and indicates that ZIF-8 has a bright future. A comparison of the adsorption capacity of Pb(II) in this study with other adsorbents reported in the literatures is shown in Table 5. It can be seemed that the Pb(II) of ZIF-8 is better than other adsorbents.

3.4. Adsorption kinetics

The adsorption kinetics for Pb(II) on the ZIF-8 surface were further analyzed by three kinds of kinetic models, pseudo-first-order kinetics model, pseudo-second-order kinetics model and Weber intra-particle diffusion model, on 200 mg/L initial Pb(II) concentration. The three kinds of kinetic model expressions are as follow:

The pseudo-first-order kinetic model[35]:

$$\log(q_e - q_t) = \log q_e - \frac{k_1}{2.303} t \quad (5)$$

The pseudo-second-order kinetic model [36]

$$\frac{t}{q_t} = \frac{1}{k_2 q_e^2} + \frac{t}{q_e} \quad (6)$$

The Weber intra-particle diffusion model [37]

$$q_t = k_{int} t^{0.5} + C \quad (7)$$

where q_e and q_t is equilibrium adsorption capacity and adsorption capacity at t min (mg/g), respectively; t (min) is contact time; k_1 (min⁻¹) is pseudo-first-order kinetic rate

Table 5

Comparison of the adsorption capacity of Pb (II) reported in the literatures and the present work

Adsorbent	Adsorbent dosage (mg/L)	C_0 (mg/L)	q_e (mg/g)	Reference
Polyaniline grafted chitosan	150	40	16.07	[29]
EPS of activated sludge	318	100	208.28	[30]
TiO ₂ /graphene oxide	250	50	53	[31]
Fe ₃ O ₄ -SO ₃ H magnetic nanoparticle	1000	10	108.93	[32]
Fe-G/RF(C)	1000	100	172	[33]
Mesoporous silica-grafted graphene oxide	100	1	255	[34]
ZIF-8	200	200	686.25	Present work

Table 6

Kinetic parameters for the adsorption of Pb(II) by ZIF-8

Kinetic model	Kinetic parameters	Pb(II)
Pseudo-first-order kinetic model	q_e (mg/g)	307.11
	K_1 (min ⁻¹)	0.0104
	R^2	0.9888
Pseudo-second-order kinetic model	q_e (mg/g)	500.00
	K_2 (g/(mg min))	0.00008
	R^2	0.9932
Intraparticle diffusion model	K_{int} (mg/(g min ^{0.5}))	18.5164
	C (mg/g)	110.4253
	R^2	0.8739

constant; k_2 (g/(mg·min)) is pseudo-second-order kinetic rate constant; k_{int} (mg/(g·min^{0.5})) is particle intra-diffusion rate constant; C (mg/g) is constant of boundary layer thickness.

Kinetics fitting results are shown in Table 6. The results indicate that the pseudo-second-order kinetic model has the best fitting effect on adsorption process for Pb(II) with ZIF-8 and R^2 is 0.9932. Fitting line of pseudo-second-order adsorption kinetic for Pb(II) with ZIF-8 is shown in Fig. 13a. The equilibrium adsorption capacity, which was calculated via pseudo-second-order model, is close to real adsorption capacity. Fitting effect of Pseudo-first-order is good and R^2 is 0.9888, but there is a significant difference between calculated equilibrium adsorption capacity and real adsorption capacity. It indicates that the pseudo-first-order kinetic model is not fitted to describe the adsorption process of Pb(II) by ZIF-8. Weber intra-particle diffusion model shows that if intra-diffusion process is the only rate controlling step, the fitting line will pass through origin. But if the line does not pass through origin, adsorption is controlled by the boundary layer in some way. If the fitting line is multiple linear relationship, the adsorption process is controlled by multiple steps [38]. As shown in Fig. 13b, the fitting line of the intra-diffusion model has two-stage and does not pass through the origin. It reveals that intra-particle diffusion is not the only determinant to control the rate as the adsorption process is controlled by out-diffusion and intra-diffusion together.

3.5. Adsorption isotherm

Adsorption isotherm shows distribution proportion of adsorbate in adsorbent and the solution, it can also reflex adsorption capacity of adsorbent to adsorbate [39]. Therefore, this experiment utilized three kinds of isotherm models, Langmuir, Freundlich and Temkin, to fit and analyze adsorption equilibrium capacity data for describing Pb(II) isotherm adsorption process by ZIF-8 in different initial Pb(II) concentration.

The Langmuir model assumes an even distribution of the adsorption sites on the surface of the adsorbent, the process belongs to monolayer adsorption, adsorbate on the surface of adsorbent are non-interacting in this case and

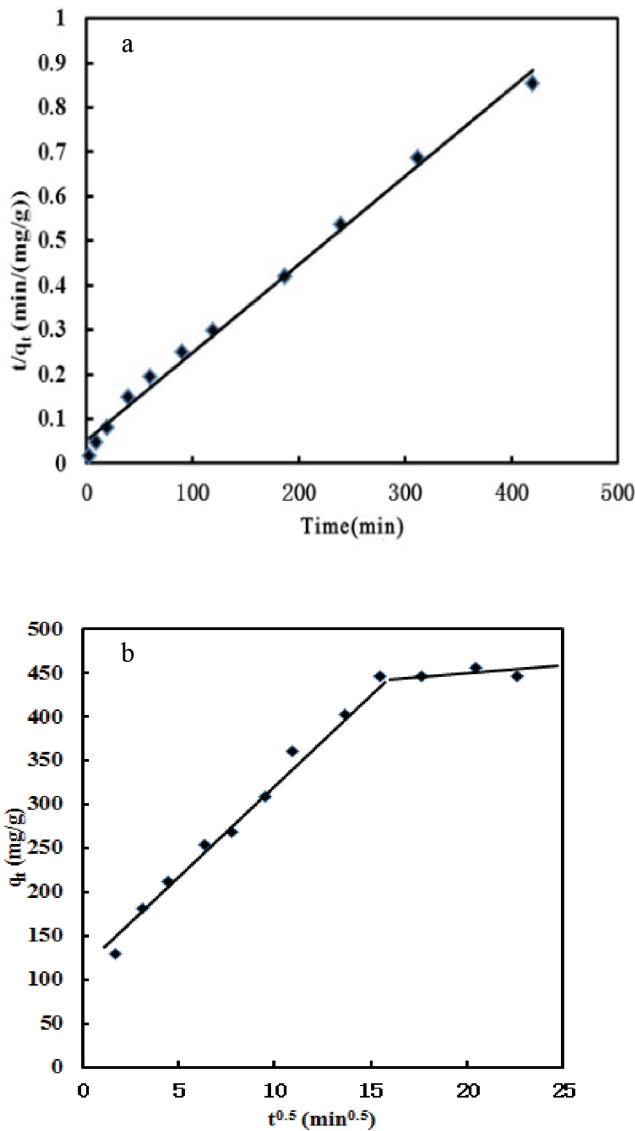


Fig. 13. Fitted line of (a) pseudo-second-order adsorption kinetic and (b) intraparticle diffusion model of Pb(II) with ZIF-8.

maximum adsorption occurs in saturation layer, which is formed by adsorbate molecule, on adsorbent surface. The model is displayed in the following equation [40]:

$$\frac{C_e}{q_e} = \frac{1}{bQ} + \frac{1}{Q}C_e \quad (8)$$

where q_e (mg/g) is equilibrium adsorption capacity for Pb(II); C_e (mg/g) is equilibrium concentration of Pb(II); Q (mg/g) is saturation adsorption capacity for Pb(II); b (L/mg) is Langmuir constant which is related with adsorption free energy. Based on the intrinsic feature of the Langmuir model, it can be judged whether the adsorption tends to be the favorable adsorption equilibrium in terms of the separation factor R_L :

$$R_L = \frac{1}{1 + bC_0} \quad (9)$$

where C_0 (mg/L) is initial concentration of Pb(II). According to the values of R_L , adsorption process can be categorized into four types: irreversible adsorption ($R_L = 0$), favorable adsorption ($0 < R_L < 1$), linear adsorption ($R_L = 1$) and unfavorable adsorption ($R_L > 1$).

Freundlich isotherm is an empirical equation describing heterogeneous surface adsorption of adsorbent by adsorbate, as shown below [41]:

$$\log q_e = \log K_F + \frac{1}{n} \log C_e \quad (10)$$

where K_F (mg/g) is Freundlich constant related to adsorption capacity, n is an intensity factor reflecting the adsorption intensity of the adsorbent.

Temkin isotherm model consider interaction of adsorbates and show that thermal energy of adsorbate molecule in the interlamination will linearly decrease with coverage area decrease due to interaction of adsorbates. The model is displayed in the following equation [42]:

$$q_e = \frac{RT}{B} \ln A - \frac{RT}{B} \ln C_e \quad (11)$$

where A (L/g) and B (J/mol) are both Temkin constants. $B = RT/b$, R (J/(mol·K)) is perfect gas constant, T (K) is thermodynamic temperature, and b (mol/J) is constant which is related with adsorption heat.

Fitting parameters of three kinds of isotherm models are shown in Table 7. It reveals that the Langmuir model has the best fitting effect on adsorption equilibrium data for Pb(II) with the highest $R^2 = 0.9827$, which the charts of linear fitting are shown in Fig. 14. It indicates that adsorption equilibrium process for Pb(II) with ZIF-8 follows the Langmuir model. Adsorption sites spread around evenly on the ZIF-8 surface and monolayer saturated adsorption capacity is 1428.57 mg/g. R_L value is 0.9618 and it reveals that Pb(II) adsorption by ZIF-8 is mainly monolayer adsorption. What's more, Temkin model

Table 7

Isotherm parameters for the adsorption of Pb(II) by ZIF-8

Isotherm model	Fitted parameters	(298K)
Langmuir	Q /(mg/g)	1428.57
	b /(L/mg)	0.00397
	R^2	0.9827
Freundlich	K_F /(mg/g)	75.0522
	n	2.4655
	R^2	0.8685
Temkin	A /(L/g)	0.09454
	B /(J/mol)	9.39162
	R^2	0.9405

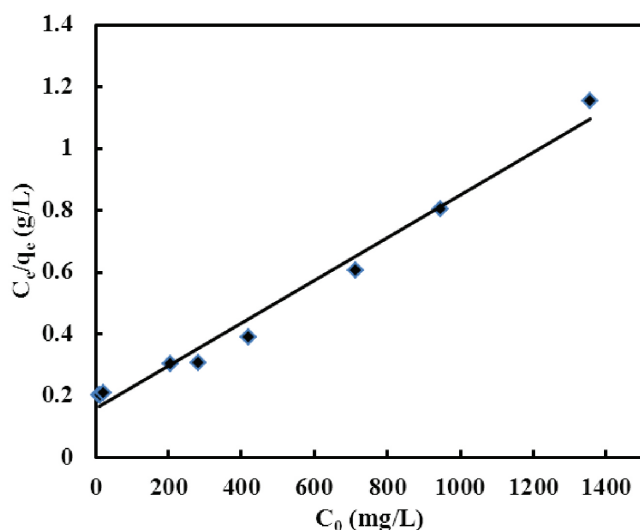


Fig. 14. Fitted line of Langmuir isotherm of Pb(II) onto ZIF-8.

also has a well-fitting effect for the Pb(II) adsorption process. R^2 is 0.9405 and Temkin model considers the interaction between adsorbates. But the fitting effect of Freundlich model is poorest and R^2 is only 0.8685. Therefore, the Freundlich adsorption isotherm model fitting effect is inaccurate.

3.6. Thermodynamics simulation

For studying the influence of temperature on the adsorption of Pb(II) with ZIF-8, thermodynamics action of 50 mg/L initial concentration solution as representative was studied. Thermodynamics parameters were calculated by the following equations [43]:

$$K_C = \frac{C_0 - C_e}{C_e} \quad (12)$$

$$\Delta G = -RT \ln K_C \quad (13)$$

$$\Delta G = \Delta H - T\Delta S \quad (14)$$

where C_0 and C_e (mg/L) are initial and equilibrium Pb(II) concentration, respectively; K_C is distribution parameter in Pb(II) adsorption equilibrium on ZIF-8 surface and solution; R (J/(mol·K)) is ideal gas constant; T (K) is absolute temperature; ΔH (kJ/mol) is enthalpy change, ΔS (J/(mol·K)) is entropy change; ΔG (kJ/mol) is Gibbs free energy change.

Thermodynamic parameters are shown in Table 8 and the thermodynamic fitting line is shown in Fig. 15. As shown in Table 8, when temperature is 283–338 K, Gibbs free energy values of adsorption reaction are all negative. The negative values indicate that the adsorption of Pb(II) with ZIF-8 is spontaneous and absolute value of Gibbs free energy increase with the decrease of temperature, which means Pb(II) adsorption by ZIF-8 will decrease with the increase of temperature. Besides, enthalpy change of adsorption for Pb(II) with ZIF-8 was -28.74 kJ/mol. This enthalpy change reveals that adsorption is an exothermic

Table 8
Thermodynamic parameters for the adsorption of Pb(II) by ZIF-8

T (K)	ΔG (kJ/mol)	ΔH (kJ/mol)	ΔS (J/mol K)	R^2
283	-8.74			
298	-7.47	-28.74	-71.34	0.9505
318	-5.36			
338	-5.12			

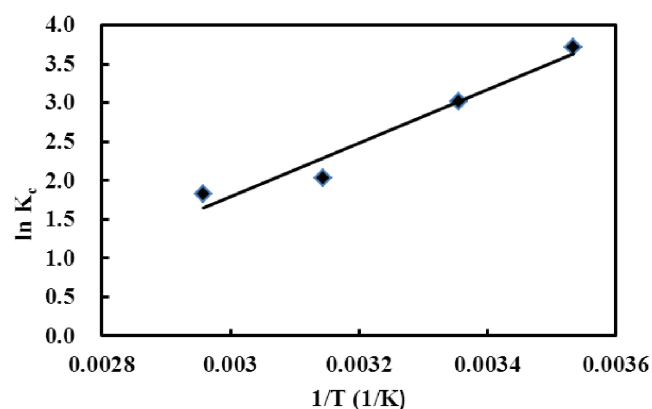


Fig. 15. Linear plots of thermodynamics for the adsorption of Pb(II) by ZIF-8.

process on ZIF-8 surface. Entropy change of adsorption process was -71.34 kJ/mol and it is entropy reduction. Because parts of degree of freedom will be lost when Pb(II) transfers from aqueous to ZIF-8 surface, it makes disorder of solid and liquid system decrease [44].

3.7. Adsorption mechanism

3.7.1. FT-IR analysis

Adsorption mechanisms were studied by infrared spectrum. The FT-IR spectra of synthetic samples are plotted in Fig. 16. There are vibration adsorption peaks at 3132 cm^{-1} and 2927 cm^{-1} , they may be elastic vibration of surface hydroxyl O–H and dissymmetrical vibration adsorption peaks of C–H bonds in the CH_3 , respectively, and the vibration adsorption peaks at 500 – 1500 cm^{-1} belong to in-plane bending vibration adsorption and stretching vibration of imidazole ring, which clarify that samples remain imidazole ring structure. Vibration peaks at 1654 cm^{-1} and 1576 cm^{-1} were caused by bend of C–N bonds and stretching vibration, respectively. In addition, the vibration peak located at 420 cm^{-1} ascribes to stretching vibration Zn–N bonds. After adsorption, there were no significant changes to vibration adsorption peaks at 421 cm^{-1} , 1653 cm^{-1} and 2927 cm^{-1} , which illuminate that C–H bonds, C–N bonds and Zn–N bonds didn't play a key role during the adsorption process. The strength of bonds at 3133 cm^{-1} become weaker, and it can be explained that hydroxyl and Lewis acid (formed by Pb(II)) react to formed compounds. The adsorption processes are shown in Fig. 17.

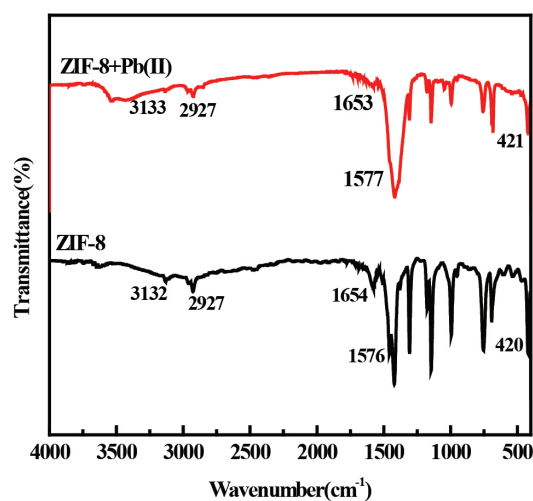


Fig. 16. FT-IR plot of ZIF-8 before and after adsorption of Pb(II).

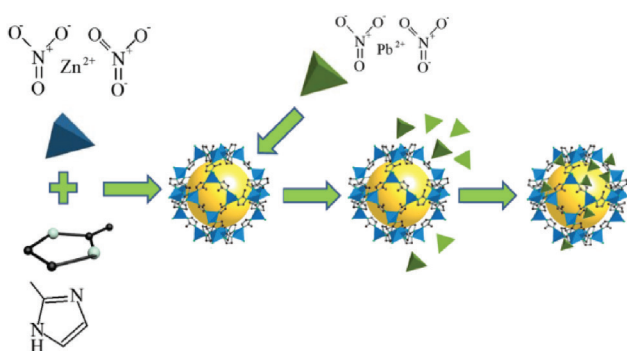


Fig. 17. Schematic diagram of Pb(II) adsorption onto ZIF-8.

3.7.2. Analysis of XPS spectra

The characteristic peaks of samples of ZIF-8 were analyzed by XPS before and after adsorption to determine the chemical states to better illuminate the adsorption mechanism. As shown in Fig. 18(a), XPS spectrogram of ZIF-8 before adsorption exist the peaks of Zn, C, O and N. However, except above elements, ZIF-8 shows clear Pb4f photoelectron line after adsorbing Pb(II). Therefore, the narrow area of Pb4f was scanned by XPS and the spectrogram of results is shown in Fig. 19b. As shown in Fig. 18b, the conjugate peak of Pb4f can be clearly observed and Pb4f_{5/2} and Pb4f_{7/2} correspond to the characteristic peak of 147.3 eV and 138.9 eV, respectively, which reveals that Pb(II) was really adsorbed by ZIF-8. Besides, as shown in Fig 18c, the binding energy of C1s and N1s are shifted. It indicates that the local bonding environments have changed [45] and it may be relate to the specific adsorption of Pb(II) on the surface of the ZIF-8 [46].

After adsorption for Pb(II), chemical environment was further studied by scan of the narrow area of Zn2p and O1s and the results are shown in Figs. 19a, b. As shown in Fig. 19a, conjugate peaks of Zn2p_{3/2} and Zn2p_{1/2} have some shift from 1022.1 eV to 1023.5 eV and from 1045.5 eV to 1047.1 eV, respectively. It reveals that Zn is a reactant in the adsorption reaction. The spectrogram of the narrow area of

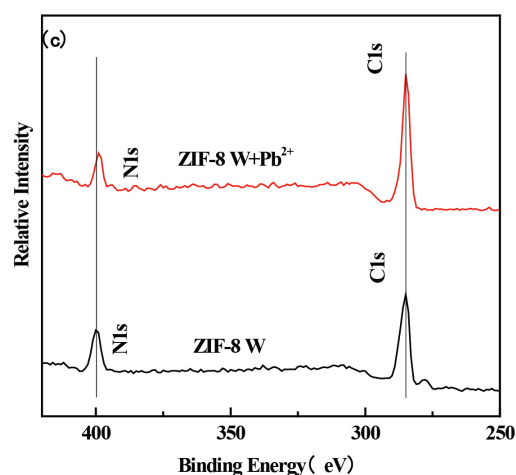
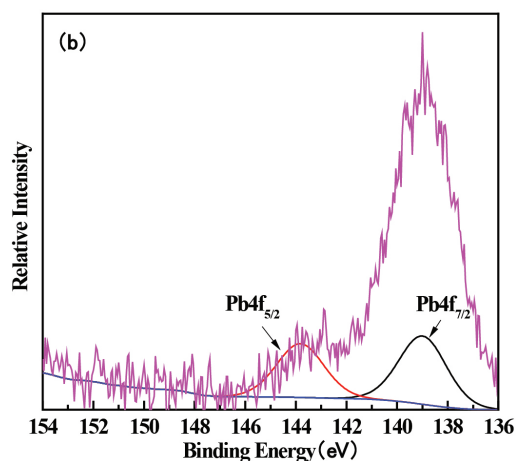
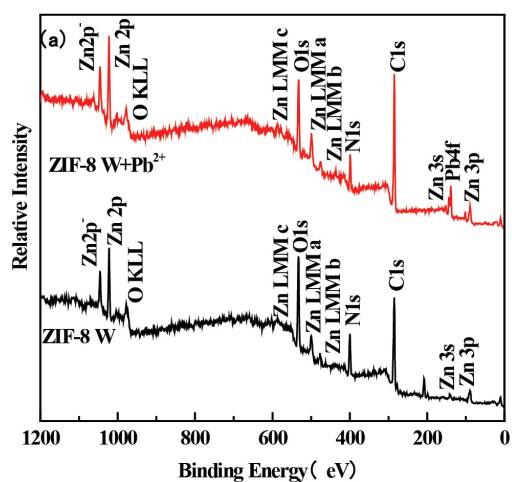


Fig. 18. (a) The spectrogram of XPS before and after Pb(II) absorption, (b) The spectrogram of XPS after Pb(II) absorption in Pb4f narrow area, (c). The XPS spectrogram of N1s and C1s before and after Pb(II) absorption.

O1s is shown in Fig. 19b, Zn-OH appeared the characteristic peak at 532.3 eV due to the presence of surface hydroxyl group before adsorption. There is a new characteristic peak of Zn-O-Pb at 534.1 eV. Clearly, the charge of Pb did not change during the adsorption process.

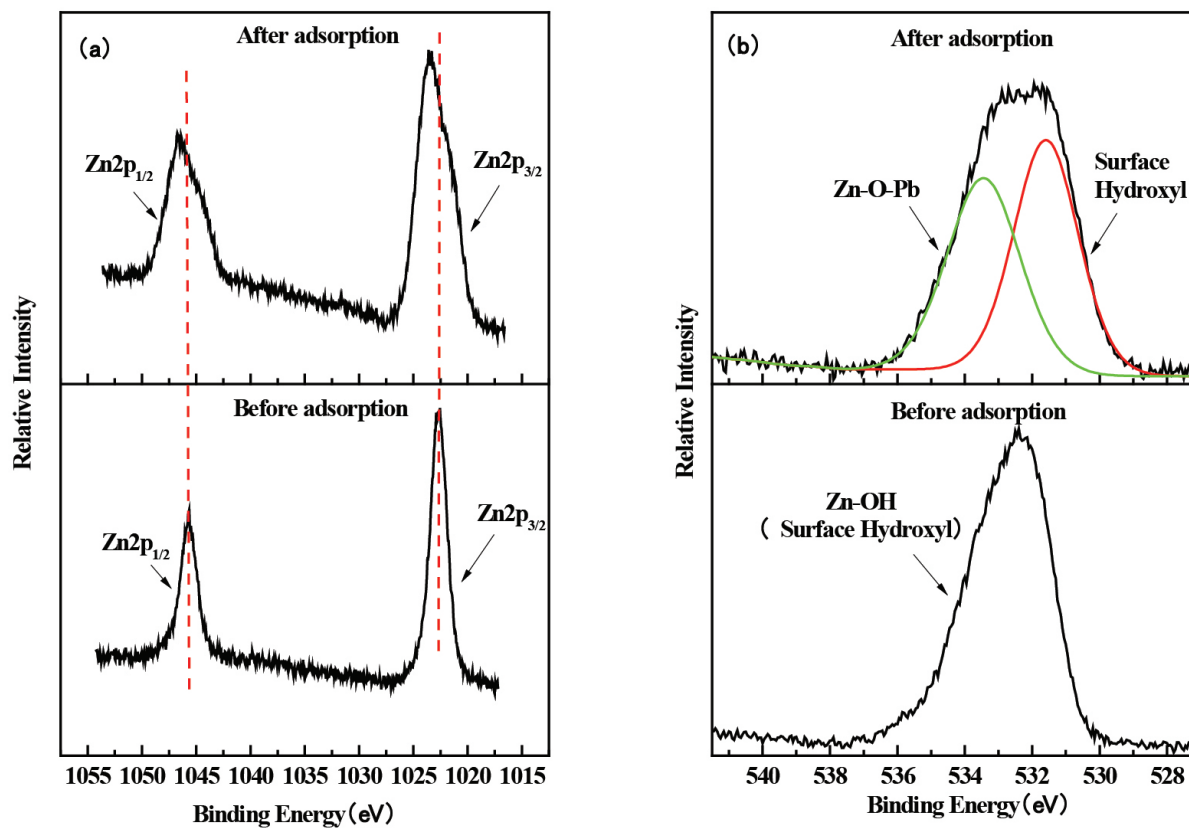


Fig. 19. (a) The spectrogram of XPS before and after Pb(II) adsorption in Zn2p narrow area. (b) The spectrogram of XPS before and after Pb(II) adsorption in O1s narrow area.

Base on the analysis of FT-IR and XPS, the possible adsorption mechanism of Pb(II) with ZIF-8 is proposed in Fig. 20. Zn–OH was formed on the surface of adsorbent due to reaction of ZIF-8 and water molecules. Zn–OH provides adsorption sites for Pb(II) and reacts with Pb(II) to form coordination compound. The Zn–O–Pb is the main interaction way for the adsorption of Pb(II) by ZIF-8.

4. Conclusion

ZIF-8 were synthesized via a simple mixing method using water as solvent, the synthetic experiments were

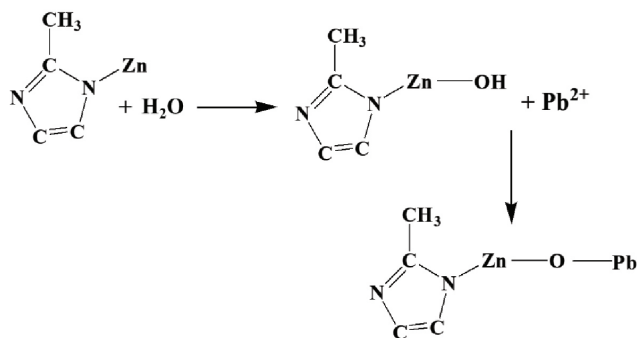


Fig. 20. Possible reaction mechanism of Pb(II) adsorption.

optimized based on central composite response surface methodology. The results reveal that solvent volume, reagent molar ratio and interaction all make significant effects. Multiple correlation coefficient reaches 0.9949. When dosage of $\text{Zn}(\text{NO}_3)_2 \cdot 6\text{H}_2\text{O}$ is 1.0 g, the optimum condition is 200 mL solvent volume and the molar ratio of H^+_{min} and Zn^{2+} is 45.63. The adsorption process of Pb(II) with ZIF-8 is spontaneous, adsorption followed the pseudo-second-order kinetic model and Langmuir model, saturated adsorption time was 4 h. When pH between 6.0–7.0, ZIF-8 showed fine adsorption effect to Pb(II). Multiply dosing method can ensure high removal capacity and effect. Adsorption capability for Pb(II) with ZIF-8 was inhibited under Ni(II) and Cu(II), especially Cu(II). Pb(II) adsorption capacity kept stable after 3 cycles. Based on the results of FT-IR and XPS, possible key mechanism of adsorption for Pb(II) is the formation of Zn–O–Pb.

Acknowledgments

The authors would like to gratefully acknowledge the financially support from the National Natural Science Foundation of China (No. 51778146), the Outstanding Youth Fund of Fujian Province in China (No. 2018J06016), the China Postdoctoral Science Foundation (No. 2014M561856), the China Scholarship Council and the Open test fund for valuable instruments and equipment of Fuzhou University (No. 2018T033).

References

- [1] Q. Zhao, Y. Wang, Y. Cao, A. Chen, M. Ren, Y. Ge, Z. Yu, S. Wan, A. Hu, Q. Bo, L. Ruan, H. Chen, S. Qin, W. Chen, C. Hu, F. Tao, D. Xu, J. Xu, L. Wen, L. Li, Potential health risks of heavy metals in cultivated topsoil and grain, including correlations with human primary liver, lung and gastric cancer, in Anhui province, Eastern China, *Sci. Total Environ.*, 470 (2014) 340–347.
- [2] F. Fu, Q. Wang, Removal of heavy metal ions from wastewaters: A review, *J. Environ. Manage.*, 92 (2011) 407–418.
- [3] Y. Yang, W. Zhang, H. Qiu, D. Tsang, J.L. Morel, R. Qiu, Effect of coexisting Al(III) ions on Pb(II) sorption on biochars: Role of pH buffer and competition, *Chemosphere*, 161 (2016) 438–445.
- [4] L. Wang, L. Yang, Y. Li, Y. Zhang, X. Ma, Z. Ye, Study on adsorption mechanism of Pb(II) and Cu(II) in aqueous solution using PS-EDTA resin, *Chem. Eng. J.*, 163 (2010) 364–372.
- [5] M. Rafatullah, O. Sulaiman, R. Hashim, A. Ahmad, Adsorption of copper (II), chromium (III), nickel (II) and lead (II) ions from aqueous solutions by meranti sawdust, *J. Hazard. Mater.*, 170 (2009) 969–977.
- [6] A. Fakhri, M. Naji, P.A. Nejad, Adsorption and photocatalysis efficiency of magnetite quantum dots anchored tin dioxide nanofibers for removal of mutagenic compound: Toxicity evaluation and antibacterial activity, *J. Photochem. Photobiol. B*, 173 (2017) 204–209.
- [7] A. Fakhri, S. Adami, Adsorption and thermodynamic study of Cephalosporins antibiotics from aqueous solution onto MgO nanoparticles, *J. Taiwan Inst. Chem. Eng.*, 45 (2014) 1001–1006.
- [8] S. Agarwal, N. Sadeghi, I. Tyagi, V.K. Gupta, A. Fakhri, Adsorption of toxic carbamate pesticide oxamyl from liquid phase by newly synthesized and characterized graphene quantum dots nanomaterials, *J. Colloid Interface Sci.*, 478 (2016) 430–438.
- [9] V.K. Gupta, A. Fakhri, S. Agarwal, A.K. Bharti, M. Naji, A.G. Tkachev, Preparation and characterization of TiO₂ nanofibers by hydrothermal method for removal of Benzodiazepines (Diazepam) from liquids as catalytic ozonation and adsorption processes, *J. Mol. Liq.*, 249 (2018) 1033–1038.
- [10] V.K. Gupta, A. Fakhri, S. Agarwal, N. Sadeghi, Synthesis of MnO₂/cellulose fiber nanocomposites for rapid adsorption of insecticide compound and optimization by response surface methodology, *Int. J. Biol. Macromol.*, 102 (2017) 840–846.
- [11] S.Z. Mohammadi, M.A. Karimi, D. Afzali, F. Mansouri, Preparation and characterization of activated carbon from *Amygdalus Scoparia* shell by chemical activation and its application for removal of lead from aqueous solutions, *Ent. Eur. J. Chem.*, 8 (2010) 1273–1280.
- [12] R. Morsy, Synthesis and physicochemical evaluation of hydroxyapatite gel biosorbent for toxic Pb(II) removal from wastewater, *Arab. J. Sci. Eng.*, 41 (2016) 2185–2191.
- [13] J. Jiang, C. Yang, X. Yan, Zeolitic Imidazolate Framework-8 for fast adsorption and removal of benzotriazoles from aqueous solution, *ACS Appl Mater Inter.*, 5 (2013) 9837–9842.
- [14] G. Fan, X. Zheng, J. Luo, H. Peng, H. Lin, M. Bao, L. Hong, J. Zhou, Rapid synthesis of Ag/AgCl@ZIF-8 as a highly efficient photocatalyst for degradation of acetaminophen under visible light, *Chem. Eng. J.*, 351 (2018) 782–790.
- [15] G. Fan, J. Luo, L. Guo, R. Lin, X. Zheng, S.A. Snyder, Doping Ag/AgCl in zeolitic imidazolate framework-8 (ZIF-8) to enhance the performance of photodegradation of methylene blue, *Chemosphere*, 209 (2018) 44–52.
- [16] S.T. Gao, W.H. Liu, N.Z. Shang, C. Feng, Q.H. Wu, Z. Wang, C. Wang, Integration of a plasmonic semiconductor with a metal-organic framework: a case of Ag/AgCl@ZIF-8 with enhanced visible light photocatalytic activity, *RSC Adv.*, 4 (2014) 61736–61742.
- [17] D.C. Montgomery, Design and analysis of experiments, Wiley, 1976.
- [18] S. Tanaka, K. Kida, M. Okita, Y. Ito, Y. Miyake, Size-controlled synthesis of zeolitic imidazolate framework-8 (ZIF-8) crystals in an aqueous system at room temperature, *Chem. Lett.*, 41 (2012) 1337–1339.
- [19] M. Rafatullah, O. Sulaiman, R. Hashim, A. Ahmad, Adsorption of copper (II), chromium (III), nickel (II) and lead (II) ions from aqueous solutions by meranti sawdust, *J. Hazard. Mater.*, 170 (2009) 969–977.
- [20] M. Jian, B. Liu, G. Zhang, R. Liu, X. Zhang, Adsorptive removal of arsenic from aqueous solution by zeolitic imidazolate framework-8 (ZIF-8) nanoparticles, *Colloid Surf. A-Physicochem. Eng. Asp.*, 465 (2015) 67–76.
- [21] X.C. Chen, Y.P. Wang, Q. Lin, J.Y. Shi, W.X. Wu, Y.X. Chen, Biosorption of copper(II) and zinc(II) from aqueous solution by *Pseudomonas putida* CZ1, *Colloid. Surface. B.*, 46 (2005) 101–107.
- [22] K. Jayaram, I.Y.L.N. Murthy, H. Lalhruiatluanga, M.N.V. Prasad, Biosorption of lead from aqueous solution by seed powder of *Strychnos potatorum* L., *Colloid. Surface. B.*, 71 (2009) 248–254.
- [23] M. Khodadadi, A. Malekpour, M. Ansaritarbar, Removal of Pb (II) and Cu(II) from aqueous solutions by NaA zeolite coated magnetic nanoparticles and optimization of method using experimental design, *Micropor. Mesopor. Mat.*, 248 (2017) 256–265.
- [24] Y. Zhang, W. Liu, L. Zhang, M. Wang, M. Zhao, Application of bifunctional *Saccharomyces cerevisiae* to remove lead(II) and cadmium(II) in aqueous solution, *Appl. Surf. Sci.*, 257 (2011) 9809–9816.
- [25] M.B. McBride, Environmental chemistry of soils, Oxford University Press, 1994.
- [26] C. Faur-Brasquet, K. Kadirvelu, P. Le Cloirec, Removal of metal ions from aqueous solution by adsorption onto activated carbon cloths: adsorption competition with organic matter, *Carbon*, 40 (2002) 2387–2392.
- [27] B.K. Jung, J.W. Jun, Z. Hasan, S.H. Jhung, Adsorptive removal of pearsanic acid from water using mesoporous zeolitic imidazolate framework-8, *Chem. Eng. J.*, 267 (2015) 9–15.
- [28] N.A. Khan, B.K. Jung, Z. Hasan, S.H. Jhung, Adsorption and removal of phthalic acid and diethyl phthalate from water with zeolitic imidazolate and metal-organic frameworks, *J. Hazard. Mater.*, 282 (2015) 194–200.
- [29] R. Karthik, S. Meenakshi, Removal of Pb(II) and Cd(II) ions from aqueous solution using polyaniline grafted chitosan, *Chem. Eng. J.*, 263 (2015) 168–177.
- [30] Y. Zhou, S. Xia, Z. Zhang, J. Zhang, S.W. Hermanowicz, Associated adsorption characteristics of Pb(II) and Zn(II) by a Novel biosorbent extracted from waste-activated sludge, *J. Environ. Eng.*, 142 (2016).
- [31] Y. Lee, J. Yang, Self-assembled flower-like TiO₂ on exfoliated graphite oxide for heavy metal removal, *J. Ind. Eng. Chem.*, 18 (2012) 1178–1185.
- [32] K. Chen, J. He, Y. Li, X. Cai, K. Zhang, T. Liu, Y. Hu, D. Lin, L. Kong, J. Liu, Removal of cadmium and lead ions from water by sulfonated magnetic nanoparticle adsorbents, *J. Colloid Interf. Sci.*, 494 (2017) 307–316.
- [33] S. Mishra, A. Yadav, N. Verma, Carbon gel-supported Fe-graphene disks: Synthesis, adsorption of aqueous Cr(VI) and Pb(II) and the removal mechanism, *Chem. Eng. J.*, 326 (2017) 987–999.
- [34] F. Aboufazel, H.R. Lotfi Zadeh Zhad, O. Sadeghi, M. Karimi, E. Najafi, Novel ion imprinted polymer magnetic mesoporous silica nano-particles for selective separation and determination of lead ions in food samples, *Food Chem.*, 141 (2013) 3459–3465.
- [35] C. Wu, Z. Xiong, C. Li, J. Zhang, Zeolitic imidazolate metal organic framework ZIF-8 with ultra-high adsorption capacity bound tetracycline in aqueous solution, *RSC Adv.*, 5 (2015) 82127–82137.
- [36] X. Jiang, H. Chen, L. Liu, L. Qiu, X. Jiang, Fe₃O₄ embedded ZIF-8 nanocrystals with ultra-high adsorption capacity towards hydroquinone, *J. Alloy. Compd.*, 646 (2015) 1075–1082.
- [37] L. Xiong, C. Chen, Q. Chen, J. Ni, Adsorption of Pb(II) and Cd(II) from aqueous solutions using titanate nanotubes prepared via hydrothermal method, *J. Hazard. Mater.*, 189 (2011) 741–748.

- [38] A. Ozcan, A.S. Ozcan, Adsorption of Acid Red 57 from aqueous solutions onto surfactant-modified sepiolite, *J. Hazard. Mater.*, 125 (2005) 252–259.
- [39] G. Fan, L. Chen, R. Lin, Q. Lin, Z. Su, X. Lin, Influence of reaction time on titanate nanomaterials and its adsorption capability for lead in aqueous solutions, *Environ. Sci.*, 37 (2016) 668–679.
- [40] L. Khezami, R. Capart, Removal of chromium(VI) from aqueous solution by activated carbons: Kinetic and equilibrium studies, *J. Hazard. Mater.*, 123 (2005) 223–231.
- [41] B. Alyuz, S. Veli, Kinetics and equilibrium studies for the removal of nickel and zinc from aqueous solutions by ion exchange resins, *J. Hazard. Mater.*, 167 (2009) 482–488.
- [42] M.J. Temkin, V. Pyzhev, Recent modifications to Langmuir isotherms, *Acta Physicochimica URSS*, 12, (1940) 217–222.
- [43] A. Ahmad, M. Rafatullah, O. Sulaiman, M.H. Ibrahim, Y.Y. ChII, B.M. Siddique, Removal of Cu(II) and Pb(II) ions from aqueous solutions by adsorption on sawdust of Meranti wood, *Desalination*, 247 (2009) 636–646.
- [44] W. Plazinski, W. Rudzinski, A. Plazinska, Theoretical models of sorption kinetics including a surface reaction mechanism: A review, *Adv. Colloid Interfac.*, 152 (2009) 2–13.
- [45] S. Guo, N. Duan, Z. Dan, G. Chen, F. Shi, W. Gao, g-C₃N₄ modified magnetic Fe₃O₄ adsorbent: Preparation, characterization, and performance of Zn(II), Pb(II) and Cd(II) removal from aqueous solution, *J. Mol. Liq.*, 258 (2018) 225–234.
- [46] C. Shen, C. Chen, T. Wen, Z. Zhao, X. Wang, A. Xu, Superior adsorption capacity of g-C₃N₄ for heavy metal ions from aqueous solutions, *J. Colloid Interface Sci.*, 456 (2015) 7–14.